This article has been accepted for publication in a future issue of this journal, but has not been fully edited. Content may change prior to final publication. Citation information: DOI 10.1109/JPHOT.2022.3173435, IEEE Photonics Journal

Optimal LED Power Allocation Framework for a Location-Assisted Indoor Visible Light Communication System

Anand Singh[+], Anand Srivastava[+], Vivek Ashok Bohara[+] and Anand Kumar Jagadeesan[*]

[+]Wirocomm Research Group, Department of Electronics & Communication Engineering
[+]Indraprastha Institute of Information Technology (IIIT-Delhi), New Delhi, India, 110020
[*]Cognizant, Chennai, India, 600096
Email: { anandsi, vivek.b, anand}@iiitd.ac.in

Abstract: The widespread deployment of white light-emitting-diodes (LEDs) for illumination provides a unique opportunity to create a flexible, accurate, and ubiquitous indoor communication and positioning system. Recent studies have shown that determining the position of a person or an object in a room can use the signals transmitted by LEDs. In this paper, we exploit the location information obtained via LEDs to improve the communication performance of an indoor visible light communication (VLC) system. Specifically, we propose an optimal LED power management framework to maximize the average data rate across the room while satisfying the bit error rate (BER) and illumination constraint across the room. The maximum allowed localization error, as a function of the number of blockages and the LED irradiance angle, have been calculated. In addition, the closed-form expression for the BER is derived for the proposed optimal LED power allocation scheme. We have also formulated an optimization problem that will maximize the power savings among the LEDs with respect to the number of blockages and permissible error in localization. It has been shown that, by employing the proposed optimal LED power allocation will results in a significant amount of power-saving, which is approximately 40% for 4 LEDs configuration and 70% for 8 LEDs configuration as compared to equal power allocation. Further, the maximum allowed localization error is found out to be approximately 7 cm and 18 cm with 4 and 8 LEDs, respectively, to achieve the maximum achievable data rate. Finally, it is shown that the dimming range of up to 70% can be achieved for the proposed system.

***Index Terms*—Visible light communication (VLC), LED power management, Power saving, Localization, Human blockage, Matern hardcore point process (MHCP).**

I. Introduction

The demand for location-assisted mobile data communication for indoor networks is increasing. According to information shared by [1]–[3], it is expected that communications data traffic will reach approximately 77 exabytes per month in the coming years, where 70% to 90% of global data traffic will occur indoor environments. The widespread use of light-emitting diodes (LEDs) for interior lighting has been an opportunity to create a whole new form of internal communication and indoor positioning system [4]–[6]. This is possible because LEDs, unlike conventional lighting, can be modulated at megahertz (MHz) frequencies and transmit data at very high speeds. Although LEDs have been classically used for indoor positioning, the use of this location information for indoor communication has yet to be explored. We believe that the acquired location estimation can be used to improve the communication performance of the system. In conjunction with positioning information, visible light communication (VLC) can provide potential solutions to problems such as static and dynamic obstacles in the indoor environment. By locating the obstacle within the LiFi attocell, the VLC parameter can be tuned to improve the overall [7], [8] communication performance. A LiFi attocell network uses the lighting system to provide wireless access to with multiple light fixtures that each function as a very small radio base station, the result is a network of very small cells that we call 'optical attocells.' They are analogous to femtocells in RF communications, which cover a small area and are, therefore, classed as 'small cells' [9]. A single room can be served by multiple optical attocells, with each covering an area of 1–10 m^2 and cell radius of about 3m.

Therefore VLC, by supplementing the existing RF communication, can provide inherent solutions to solve the problems confronted by RF communication in an indoor environment [8] [7]. Intensity modulation / direct detection (IM/DD) is a primary operating principle of VLC, where light intensity from the transmitting light-emitting-diode (LEDs) is used to modulate the information signal [10]–[12] which can be received at the photodetectors and converted into an electrical signal. Moreover, LED sources serve the dual role of illumination and communications which could result into considerable power savings. It is also prone to significant power losses due to blockages [13]. In an indoor environment, the communication performance is hampered by various factors such as stationary blockages like furniture, the movement of the other users, which may act as an obstacle to the desired user [14]. Furthermore, in an communication system, the user terminals (UT) are usually mobile, adding randomness to the channel between the access point (AP) and the UT. However, despite the advantages mentioned above, it has some disadvantages, such as it suffers from high interference from other light sources and significant blockage losses due to shadowing [15].

In an indoor VLC system, the received optical power depends on various factors, such as the location of the emitting LEDs, the desired user's location, and the different types of obstacles present in the room. In an indoor room with multiple-user cases, other users act as a blockage for the desired user. Sometimes other users may pause between movements for a specific time, called a pause time. These pauses taken by

This article has been accepted for publication in a future issue of this journal, but has not been fully edited. Content may change prior to final publication. Citation information: DOI 10.1109/JPHOT.2022.3173435, IEEE Photonics Journal

moving users can obstruct line-of-sight (LoS) and non-line-of-sight (NLoS) signals from the transmitter to the receiver, and hence can abruptly drop the received power. The height and the radius of the blockages play a significant role in this sudden reduction of the received power [16]. Consequently, the motivation behind this work is to exploit the location information obtained in the presence of obstacles to facilitate better communication services meeting BER better than 10^{-3} and illumination in the range of 300-1500 lux [17], [18].

A. Related Work

Previous studies have shown that it is necessary to study the impact of obstacles and user location for an indoor VLC system. Various positioning models have been used to characterize a user's location in an enclosed area. A novel indoor location system is presented in [19], where the user's position is determined using LED beacons. As part of the existing lighting infrastructure, LEDs transmit their IDs over long distances using VLC. The positioning method uses new geometric and consensus techniques, which tolerate measurement inaccuracies, and system performance is analyzed using simulations and precise measurements. According to performed tests in realistic environments, the accuracy of the approach is in the lower decimeter range. However, their work has not studied the problem of failures in visible light positioning (VLP) systems. To overcome the above drawback. Anastou et al., in [20] presented a low complexity VLP with sinusoidal wave forms allowing the use of a large number of LEDs for localization. Additionally, to address the acquired signal's low signal-to-noise ratio (SNR), they present the concept of duplicating the location estimate for a small number of overlapping received signal segments that vary by a small number of samples. The resultant positions are averaged to generate the final estimation. In [21] and [22] authors review the optimization techniques previously reported in the literature to improve the VLC network performance when the system consists of multi-users. Four main issues are considered in this type of network, for maximizing the various objectives and achieving the various constraints, including power and resource allocation, users-to-APs association, cell formation, and AP cooperation used for mitigating the disadvantages of VLC networks to improve performance.

In [23], a typical application of VLC by designing a three-dimensional positioning scheme for a target terminal equipped with several photodiodes (PDs) is proposed. Given the relative coordinates between the receiving PDs and the fixed transmitting LEDs, an accurate estimate of the terminal's location can be obtained by estimating RSS through LoS channels. Additionally, it is shown that the multipath reflections from walls are significant interference in an NLoS environment. It can be seen that the positioning error grows linearly with the reflection coefficient of the walls, which is also verified using simulation results. In [24], the authors discuss both active and passive positioning schemes where the active positioning consists of tracking a tag attached to or carried by the target. On the other hand, passive positioning involves positioning a target without a device or untagged. Although passive or devices location is relatively more challenging to achieve, it is preferred for many applications. The work in [24] provides detailed insight into discrete passive positioning facilitated by non-RF sensing techniques. Bai et al., in [25] proposed a new VLC-assisted four-line perspective algorithm (V-P4L) for indoor localization. The basic principle of V-P4L is to jointly use the coordinate information obtained by VLC and the geometric information in computer vision for a convenient indoor location. In [26], the authors presented a unique indoor positioning paradigm named area-based positioning, in which various-angle optical user devices position themselves for low-cost, fixed-location active photovoltaic anchors. Cincotta et al., in [27] show that the introduction of luminaire reference points (LRPs) dismisses this limitation and allows the creation of a self-contained VLP system that requires only a single luminaire in its field-of-view (FOV). It is noted that the models presented in the existing literature focus on optimizing the location accuracy. Employing this location information to improve communication performance has been ignored. Also, how can we use this location information to improve the shadowing caused by obstacles inside the room.

Earlier authors review the optimization techniques previously reported in the literature to improve the VLC network performance when the system consists of multiple users. In [10], authors considered four main issues are considered in this type of network, for maximizing the various objectives and achieving the various constraints, including power and resource allocation, users-to-APs association, cell formation, and AP cooperation used for mitigating the disadvantages of VLC networks to improve performance. Similarly, in [28], with the help of a central controller, and by considering the arbitrary receiver orientation, Soltani et al. proposed an approach for APA to users, based on the strength of the received signal and the traffic of the APs, aimed at maximizing the system's throughput. It is shown that, when a any user wants to join an network, the central controller calculates all the offered data rates from all APs and enables the user to select the best AP. Wu et al. in [29], jointly allocated time resources to the users and assigned APs to the users. They considered the resource allocation problem as a bidirectional allocation game, since the aim of APs is to select the only users that maximize the system throughput, and the users want to select APs providing better QoS. By considering mobile users in standalone VLC networks, Zhang et al. in [30], proposed a novel user-to-AP assignment based on anticipating the future users' locations and their traffic dynamics, and find a trade-off between the delay and the throughput in the dynamic VLC systems. Jiang et al. in [31], studied and formulated the joint power allocation and LB problems. Chen et al. in [32], investigated the effects of the cell size and network deployment on the performance of VLC systems by measuring the signal-to-noise and interference ratio (SINR) distributions.

In the proposed work, as suggested in clinical studies [33], [34], while calculating the optimal LED power allocation based on the user's locations (also the blockers) inside the room, we have make sure that, for each attocell, even if there is no user inside that attocell, the minimum illumination level (300 lux) is maintained. In this paper, to maintain illumination

This article has been accepted for publication in a future issue of this journal, but has not been fully edited. Content may change prior to final publication. Citation information: DOI 10.1109/JPHOT.2022.3173435, IEEE Photonics Journal

and communication, we have used the concept of dedicated illumination streams along with communication streams. Two streams independently perform the task of illumination and communication [(I1 streams) illumination + (I2 streams) communication]. This concept achieves and maintains the illumination targets while also supporting desired communication.

B. Contribution

As evident from above, the existing work on VLP primarily focused on minimizing the error in localization by exploiting different positioning methods. Further, in earlier work, utilization of this location information for indoor communication has not been explored. We believe that this position information can be exploited to improve communication performance in the presence of different obstacles inside the room. Moreover, the LED power allocation can be optimized to maximize the data rate or minimize the BER by exploiting this location information. The proposed work has the following major contributions.

1) We propose a location-assisted indoor VLC system, wherein the location information is exploited to enhance the communication performance of the user. Specifically, we propose an optimal LED power management scheme to maximize the average data rate across the room subject to predefined communication constraints as well as number of blockages inside the room.
2) We have also formulated a power-saving optimization framework to maximize the power savings among the LEDs with respect to the number of blockages and permissible localization error. The effect of dimming on the above is also investigated.
3) The closed-form expression of BER for optimal LED power allocation with blockages and localization is derived.
4) Further, to see the effect of a high rate modulation scheme in the proposed system model, we have analyzed the BER performance and the localization error with DCO-OFDM and human blockage. The effect of random device orientation on the BER performance is also analyzed.
5) In addition, we have also analyzed the trade-off between the localization error and the performance metrics such as BER and illumination for the proposed location-assisted indoor VLC system.

The rest of this paper is organized in the following way. Section II presents the system model, consisting of the VLC system model and the characterization of the dynamic human blockages using generalized MHCP. In Section III, we have discussed the proposed optimal LED power allocation employing user location. We explain the shadowing effect and develop a model to find the blockage probability for any dynamic user in the indoor VLC system. The analytical expression for received power and BER is discussed in Section IV. Section V discusses the analytical as well as the simulation plots. Lastly, Section VI concludes the entire article.

II. System Model

The system model considers 4 LEDs transmitters placed in the rectangular configuration in a room size of $x \times y \times z$ (m $\times$ m $\times$ m). The receiver plane is at the height of 0.85 m. Generalized RWP model (with pause time t_p) has been employed to characterize the distribution of dynamic blockages in a space $[x, y]^2$. The human blockages are modelled as cylinders of height h_B and radius r_B, as shown in Fig.1. For the given system model, blockages of different widths (radius r_1 and r_2) have been considered to replicate the different sizes of people. Since on-off keying (OOK) modulation is a standard modulation scheme outlined in the VLC standard (IEEE 802.15.7) [R10], we use OOK modulation in the proposed VLC system for determining the power and signal-to-noise (SNR) expression. Also, to see the effect of state-of-the-art high data rate modulation schemes such as DCO-OFDM on the proposed LED power allocation framework, we have analyzed the BER performance, and the maximum allowed localization error using DCO-OFDM [35].

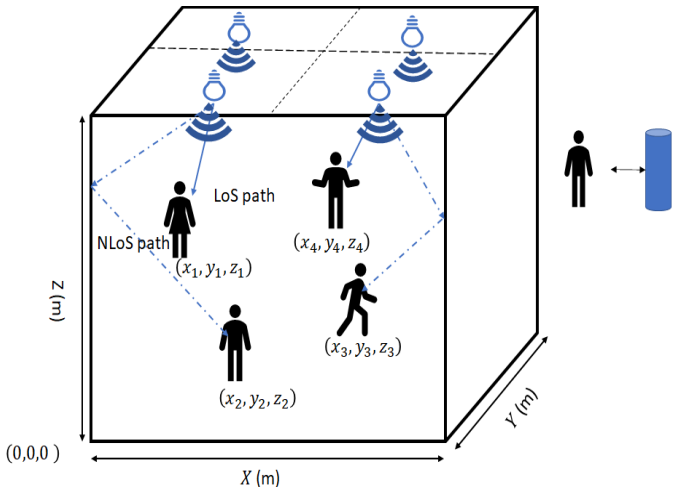

Fig. 1. Indoor Visible light positioning system with human blockages

The proposed system model can be generalized to a room of any arbitrary size. However, for ease of analysis and without the loss of generality, we consider a square room size of $5 \times 5 \times 3$ (m $\times$ m $\times$ m), where the LEDs 1, 2, 3, and 4 are placed at the height of 3m at (1.25, 3.75), (3.75, 3.75), (1.25, 1.25), (3.75, 1.25) respectively. It is assumed that the location information of the human blockages is available beforehand by utilizing the methods discussed in Section I.

In the following sub-sections, we discuss in detail the multipath VLC channel, the modeling of human blockages using MHCP, and the effect of shadowing.

A. VLC Channel Model

In this article, we have used a multipath VLC channel model with second-order reflection. Lambertian model is a well-established radiation model that can model the radiation of the LED light source in VLC. Also, the given Lambertian model can precisely reproduce both the LoS and NLoS light intensity transmitted by LED [14]. Therefore, the overall VLC channel gain is a sum of both the LoS path (direct path between the LED and the user) and the NLoS path reflected by the walls,

This article has been accepted for publication in a future issue of this journal, but has not been fully edited. Content may change prior to final publication. Citation information: DOI 10.1109/JPHOT.2022.3173435, IEEE Photonics Journal

as shown in Fig. 1. The channel gain of LoS component H_{LoS}, is given as:

$$H_{LoS} = \begin{cases} \dfrac{(m+1)A}{2\pi D^2}\cos^m(\phi)T_s g(\psi)\cos(\theta) \\ \qquad\qquad 0 \le \Psi \le \Psi_c \end{cases} , \tag{1}$$

where m represents Lambertian order defined as:

$$m = \frac{-\ln(2)}{\ln(\cos(\Phi_{\frac{1}{2}}))} . \tag{2}$$

Here, A represents the physical area of the PD, θ is the angle of incidence to the PD from LED, ϕ is the LED angle of irradiance, ψ_c is the receiver FOV, $T_s(\psi)$ is the optical filter's gain, D_d is the distance between the VLC transmitter (LED) and the receiver (PD), and $g(\psi)$ is the optical concentrator's gain given as:

$$g(\psi) = \begin{cases} \dfrac{n^2}{\sin^2(\Psi_c)}, & 0 \le \Psi \le \Psi_c, \end{cases} \tag{3}$$

where n is the optical concentrator's refractive index and $\phi_{\frac{1}{2}}$ is LED semi angle. The NLoS channel gain is defined as:

$$H_{NLoS}^{wall} = \begin{cases} \dfrac{\rho(m+1)A}{2\pi D_1^2 D_2^2}\cos^m(\phi)T_s(\psi)g(\psi) \\ \qquad \cos(\alpha_{wall})\cos(\beta_{wall}) \\ \qquad\qquad 0 \le \Psi \le \Psi_c \end{cases} , \tag{4}$$

Here α_{wall} and β_{wall} are the incidence and reflectance angle non-line of sight link make with reflecting surface (wall) have reflection coefficient ρ. D_1, D_2 are the distance traveled by the NLoS link to reach the user from the wall.

The total received power using multiple LEDs including both LoS as well as NLoS path through the walls for a given transmission power (P_T), can be expressed as:

$$P_r = \sum_{i=1}^{N}\left[P_T H_{LoS} + \sum_{k=1}^{K} P_T H_{NLoS}\right] , \tag{5}$$

Here, N is the number of transmitting LEDs, and the total received power is obtained by summation both LoS the NLoS link from the walls across the room.

B. Modeling of human blockages using MHCP

In this paper, we have used Matern Hard Core Process (MHCP) to generate multiple objects in an indoor environment. Hard-Core processes are point processes where points are not allowed to be closer than a certain minimum distance. Thus, they are more regular (less clustered) than other point processes. Moreover they realistically emulate real-life scenarios where objects have a finite width and cannot occupy the same space. In this paper, we have MHCP Type-II, where we start with a basic uniform Poisson point process (PPP) ϕ_b with intensity λ_b, and then remove all points which have another point within the minimum distance r. The intensity of the resulting process is [36]:

$$\lambda_{B1} = \frac{1-\exp(\lambda_p \pi \delta^2)}{\pi\delta^2}. \tag{6}$$

where λ_p is the intensity of the parent point process.

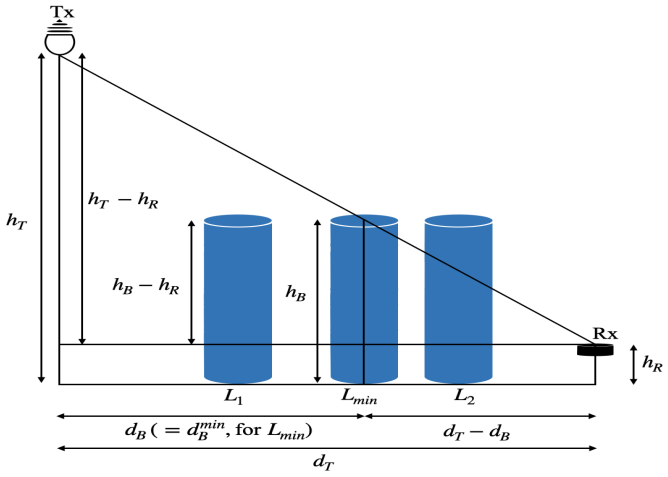

Fig. 2. Schematic for calculation of minimum blockage distance

C. Shadowing Effect

In a practical multi-user scenario, the other users inside the room act as blockages for the desired user. These blockages result in a sudden fall in the received optical power as it can block both the LoS and the NLoS signal from the LED to the desired user. The amount of power reduction will depend on the height and width of the blockage. In this paper, in order to calculate the effect of shadowing due to obstacles on the received power, we have calculated the probability of the VLC channel link getting blocked due to the presence of an obstacle at a distance of d. So, whenever an obstacle occurs in the LoS path between any Tx and the Rx, a shadow of that obstacle will be formed. Since the blockages are cylindrical, it is assumed that the shadow is rectangular. If the length of the shadow is long enough to fall on the receiver, it might result in a communication link obstruction between that particular Tx and Rx. This is known as the Shadowing Effect. A blockage has to be in a specific region (known as the shadow region) to hamper the Tx-Rx link. The potential human blockages are distributed over the receiver plane. As stated before, we model the blockages as cylinders with a certain height, h_B, and the base diameter of D. The locations of the human blockages present inside the room are distributed as per the mobility aspects of humans [15]. We will derive this condition shortly. Those length is $d_T - d_B$ will fall on the Rx if the distance between the blockage and the base of the Tx will be greater than d_B^{min}. Otherwise, the light will pass over the blockage, and no communication link blockage would be observed (as depicted by the blockage present at the location L_1 in Fig. 2). Using simple trigonometry, from Fig. 2, we get:

$$d_B = d_T.\left(\frac{h_T - h_B}{h_T - h_R}\right) \tag{7}$$

Similarly, the probability that the center of at least one blocking object falls in the shadow area can be calculated using the void probability [37] [16]:

$$P_B(d) = 1 - \exp\left(-2\lambda_{B1} d_B r_B^2\right). \tag{8}$$

where λ_{B_1} is the blockage intensity having same radius and r_B is the blockage radius which can be either r_1 or r_2.

Further, if there is human blockage between the LED and the PD at distance d with probability $P_B(d)$, the VLC channel gain with blockage can be expressed as:

$$\begin{aligned} H_{i,j}^B &= H_{ij}\left[(1-P_B(d))\right] \\ &= \frac{M[\exp\left(-2\lambda_B d_{i,j} r_B^2\right)]}{2\pi d_{i,j}^2}, \end{aligned} \tag{9}$$

where $M = (m+1)\cos^m(\phi) A \cos(\theta)$.

III. LED power allocation Optimization problem (To Maximize achieved data rate)

This section proposes the optimal LED power management framework based on human blockage estimation inside the room. The objective is to maximize the average bit rate among the users subject to the illumination and BER constraints. Here, we consider multiple LEDs and multiple user scenario wherein each user will act as a human blockage to others. The average bit rate is the function of the average received signal-to-noise ratio (SNR) at the receiver in the presence of human blockages [38]. The average bit rate is maximized by optimally allocating the transmit power P_{t_i} among LEDs and can be expressed as:

$$\max_{P_{t_i}} \ \log_2\left[1+\mathbb{E}\left[\frac{\left(\mathcal{R}\sum_{i=1}^{N} H_{i,j}^B P_{t_i}\right)^2}{\sigma_j^2}\right]\right] \tag{10}$$

$H_{i,j}^B$ is the VLC channel coefficient between i^{th} LED and j^{th} PD in the presence of human blockages and σ_j^2 is the noise variance at j^{th} PD. The objective function is subjected to following constraints:

1) The sum of power of each LED is upper-bounded by P_T

$$\begin{aligned} &\sum_{i=1}^{N} P_{t_i} \le P_T, \\ &\Rightarrow 1_N \mathbf{x} \le P_T. \end{aligned} \tag{11}$$

where, 1_N is a N dimensional unit vector and $\mathbf{x} = [P_{t_1}, ..., P_{t_N}]^T$ is N dimensional column vector of decision variables.

2) The power of each LED is non-negative.

$$P_{t_i} \ge 0 \quad \forall i = 1, ..., N, \tag{12}$$

$$\Rightarrow \mathbf{G}\mathbf{x} \ge 0. \tag{13}$$

where $\mathbf{G} = \mathrm{diag}(1, ..., 1)$.

3) BER should be $P_e \le 10^{-3}$

$$Q\left(\sqrt{\frac{\left(\mathcal{R}\sum_{i=1}^{N} H_{i,j}^B P_{t_i}\right)^2}{\sigma_j^2}}\right) \le 10^{-3}. \tag{14}$$

4) The illumination across the room must be within a predefined range

$$1500 \ \ \text{lux} \ge \left[\frac{P_{t_i}\cos^{m+1}(\phi)\cos(\theta)}{4\pi r^2}\right] \ge 300 \ \ \text{lux} \tag{15}$$

where r is the attocell radius.

The second term inside the log function in optimization function (10) is the expected SNR at the receiver in the presence of blockage and can be calculated as:

$$\mathbb{E}\left[\frac{\left(\mathcal{R}\sum_{i=1}^{N} H_{i,j}^B P_{t_i}\right)^2}{\sigma_j^2}\right] = \mathcal{R}^2\mathbb{E}\left[\left(\frac{P_{r_j}}{\sigma_j^2}\right)^2\right], \tag{16}$$

$$\begin{aligned} \mathcal{R}^2\mathbb{E}\left[\left(\frac{P_{r_j}}{\sigma_j^2}\right)^2\right] &= \mathcal{R}^2\mathbb{E}\Bigg[\frac{\sum_{i=1}^{N}\left(H_{i,j}^B\right)^2 P_{t_i}^2}{\sigma_j^2} \\ &\quad + 2\frac{\sum_{i=1}^{N}\sum_{q=i+1}^{N} H_{i,j}^B H_{q,j}^B P_{t_i} P_{t_q}}{\sigma_j^2}\Bigg] \\ &= \mathcal{R}^2\Bigg[\frac{\sum_{j=1}^{K}\sum_{i=1}^{N}\left(H_{i,j}^B\right)^2 P_{t_i}^2}{K\sigma_j^2} \\ &\quad + \frac{\sum_{j=1}^{K} 2\sum_{i=1}^{N}\sum_{q=i+1}^{N} H_{i,j}^B H_{q,j}^B P_{t_i} P_{t_q}}{K\sigma_j^2}\Bigg], \\ &= \mathcal{R}^2\left[\frac{\sum_{i=1}^{N}\mu_{i,i}^B P_{t_i}^2 + 2\sum_{i=1}^{N}\sum_{q=i+1}^{N}\mu_{i,q}^B P_{t_i} P_{t_q}}{K\sigma_j^2}\right], \end{aligned} \tag{17}$$

where $\mu_{i,q}^B = \sum_{j=1}^{K} H_{i,j}^B H_{q,j}^B$ and K is total number of PD. By substituting the value of received SNR in (10) the average data rate for N_u users can be expressed as:

$$\begin{aligned} \log_2\left[1+\frac{\left(R\sum_{i=1}^{N} H_{i,j}^B P_{t_i}\right)^2}{\sigma_j^2}\right] &= \log_2\left[1+\mathcal{R}^2\mathbb{E}\left[\left(\frac{P_{r_j}}{\sigma_j^2}\right)^2\right]\right] \\ &= \frac{1}{N_u}\left[P_{t_1,...,P_{t_N}}\right] \\ &\quad \begin{bmatrix} \beta_{11} & ... & \beta_{1N} \\ .. & .. & .. \\ \beta_{N1} & .. & \beta_{NN} \end{bmatrix} \begin{bmatrix} P_{t_1} \\ .. \\ P_{t_N} \end{bmatrix}, \end{aligned} \tag{18}$$

Using (10) and (18), the proposed optimization problem can be expressed in matrix form as:

$$\max_{x} \ \frac{1}{N_u}\mathbf{x}^T\mathbf{B}\mathbf{x}, \tag{19}$$

where the matrix $\mathbf{B}$ is given by

$$\mathbf{B} = \begin{bmatrix} \beta_{1,1} & ... & \beta_{1,N} \\ .. & .. & .. \\ \beta_{N,1} & .. & \beta_{N,N} \end{bmatrix}. \tag{20}$$

and elements $\beta_{i,q}$ are

$$\beta_{i,q} = \left[\frac{\sum_{i=1}^{N}\mu_{i,i}^B P_{t_i}^2 + 2\sum_{i=1}^{N}\sum_{q=i+1}^{N}\mu_{i,q}^B P_{t_i} P_{t_q}}{K\sigma_j^2}\right], \tag{21}$$

This article has been accepted for publication in a future issue of this journal, but has not been fully edited. Content may change prior to final publication. Citation information: DOI 10.1109/JPHOT.2022.3173435, IEEE Photonics Journal

The objective function in (18) is convex because $\mathbf{B}$ is positive-definite [39]. Since the variance of received power $\mathbf{x}^T\mathbf{B}\mathbf{x} > 0 \ \forall \ \mathbf{R}_+^N$, $\mathbf{B}$ is positive-definite. Also, the linear functions are both convex and concave, and all constraints are convex. Therefore, the optimization problem in (10) gives a quadratic and the convex optimization problem.

A. Power saving optimization

In this sub-section, we formulate an optimization problem to maximize the power saving among the LEDs based on localization information. The optimization problem also takes into account the human blockages inside the room. Specifically, we derive the total power to be distributed among the LEDs based on the optimal LED power management framework described in Section III in order to fulfill both illumination and BER constraints. The objective power saving function is the total allotted power based on equal power allocation to all the LEDs subtracted from the total allocated power (using optimal LED power allocation framework), fulfilling both illumination and BER constraints, i.e.,

$$\max_{N_B} \quad [P_T - P_A], \tag{22}$$

Here, P_A the minimum required allocated power to the LEDs for a given number of blockages using the proposed optimal LED power allocation scheme. P_T the total power required with equal power allocation to maintain the constraints like, average BER should be $\leq 10^{-3}$. The illumination across the room should be $1500 \ \text{lux} \geq I_{avg} \geq 300 \ \text{lux}$. The total power constraint of the system being $\sum P_{t_i} \leq P_T$.

IV. BER PERFORMANCE

In this section, we analyze the BER of the VLC channel in the presence of dynamic blockages characterized by MHCP.

To calculate the blockage probability $P_B(d_B)$, it is assumed that no signal is received whenever the PD is blocked by the obstacle. The optical signal $s_i(t)$ transmitted by the i_{th} LED is as follows:

$$s_i(t) = P_{t_i}[1 + M_I x_i(t)], \tag{23}$$

where P_{t_i} is the i_{th} LED's the transmit power, M_I is the modulating index and $x_i(t)$ is the corresponding OOK modulated signal [40]. The first term in (23) (P_{t_i}) accounts for the illumination whereas the second term $(P_{t_i} M_I x_i(t))$ for the communication part. It is assumed that the DC component of the detected electric signal is filtered out at the Rx after photo detection. y_j is the received signal at the photo-detector j, and is expressed as:

$$y_j = \mathcal{R} P_{r_j} + n_j, \tag{24}$$

where $\mathcal{R}$ is the responsivity of the PD and n_j is the additive white Gaussian noise (AWGN) with zero mean and σ_j^2 variance. Thus, we can write the AWGN as $n_j = \mathcal{N}(0, \sigma_j^2)$. Received power at the j^{th} photo-detector, P_{r_j} is given by:

$$P_{r_j} = \sum_{i=1}^{N} H_{i,j}^B P_{t_i} M_I x_i. \tag{25}$$

$$P_{r_j} = \sum_{i=1}^{N} \frac{P_{t_i}(m+1)Ah_T^{m+1} M_I x_i [\exp\left(-2\lambda_B d_{i,j} r_B^2\right)]}{2\pi \left(\sqrt{h_T^2 + r_i^2}\right)^{m+3}}, \tag{26}$$

Here, h_T is the height of transmitter plane and r_i location of the i^{th} LED from the centre. As we know the location of blockages, as well as that of the PD, the transmitting power from the LED, will be given by vector $P_{t_i} = B_i P_T$ get from (19) the optimal LED power allocation.

$$P_{r_j} = \sum_{i=1}^{N} \frac{B_i P(m+1)Ah_T^{m+1} M_I x_i [\exp\left(-2\lambda_B d_{i,j} r_B^2\right)]}{2\pi \left(\sqrt{h_T^2 + r_i^2}\right)^{m+3}}, \tag{27}$$

where B_i is the i_{th} LED power allocation vector derived using optimization in (25). Let,

$$C_1 = \frac{P(m+1)Ah_T^{m+1}}{2\pi}, \tag{28}$$

and

$$V_i = \frac{B_i x_i [\exp\left(-2\lambda_B d_{i,j} r_B^2\right)]}{\left(\sqrt{h_T^2 + r_i^2}\right)^{m+3}}. \tag{29}$$

Now P_{r_j} can be expressed as:

$$P_{r_j} = C_1 \sum_{i=1}^{N} V_i, \tag{30}$$

Hence the output signal can be written as:

$$y_j = \mathcal{R} C_1 \sum_{i=1}^{N} V_i + n_j, \tag{31}$$

Here n_j is the noise σ_j^2 at j^{th} the PD is the total noise power comprising of shot noise power (σ_{shot}^2) and thermal noise power $(\sigma_{\text{thermal}}^2)$ which can be expressed as:

$$\sigma_j^2 = \sigma_{\text{shot}}^2 + \sigma_{\text{thermal}}^2. \tag{32}$$

Using (31), the BER for OOK modulation scheme with the optimal LED power allocation with human blockages can be expressed as:

$$P_e = Q\left(\frac{\mathcal{R} C_1 \sum_{i=1}^{N} V_i}{\sigma_j}\right). \tag{33}$$

V. RESULTS AND DISCUSSION

In this section, the simulation and analytical results for the proposed indoor VLC broadcast system inside a standard room sizes of $5 \text{ m} \times 5 \text{ m} \times 3 \text{ m}$ and $10 \text{ m} \times 10 \text{ m} \times 3 \text{ m}$ have been presented. Each room consists of either 4 and 8 LED transmitters placed in a rectangular geometry. A Monte Carlo simulation of 10^4 independent trials is conducted, where for each trial, a random location of blockages has been generated. The locations of the VLC transmitters, receiver and the orientations are provided in Table I.

This article has been accepted for publication in a future issue of this journal, but has not been fully edited. Content may change prior to final publication. Citation information: DOI 10.1109/JPHOT.2022.3173435, IEEE Photonics Journal

TABLE I
SYSTEM MODEL PARAMETERS

Ref.	System Model
Total transmitted power P_T	200 mw
Refractive index n	1.5
Optical filter gain T_s	1
Wall reflection ρ	0.8
Number of user N_u	1-8
Number of receiver location K	625
LED semiangle Φ	60°
Receiver plane above the floor h_R	0.85 m
Receiver elevation	90°
Receiver active area A	1 cm^2
FOV of the receiver ψ_c	60°
Blockage radius r_1 and r_2	20 cm & 40 cm
Height of the blockage h_B	180 cm
Responsivity $\mathcal{R}$	0.5 $\frac{A}{W}$
Signal bandwidth B_s	10 MHz
Noise bandwidth factor I_2	0.562
Background current I_{bg}	100 μA

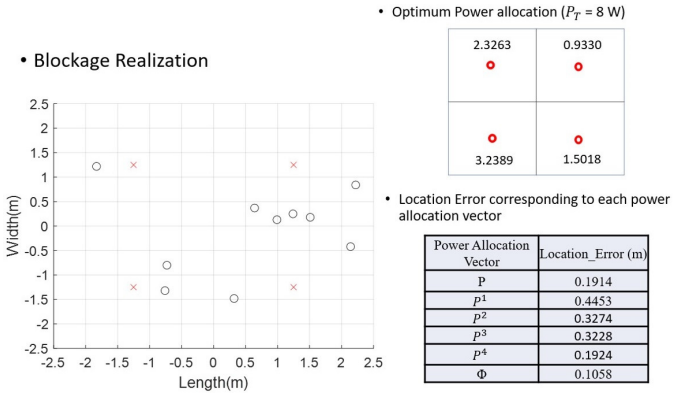

Fig. 3. Position of objects, power allocated to the LED's and the location error

A. Location Estimation and Complexity of the system

In the proposed optimal LED power allocation framework, in order to update the LED power in real-time with respect to the user's location inside the room, we require estimation of the user location, which is further fed into the LED controller, which distributes the power among LEDs as per the proposed optimal LED power allocation. Here we can use a microcontroller-based LED controller circuit to facilitate the power management (varying light intensity) of the LEDs based on the user's location information inside the room.

Here we present how the location estimation can be incorporated into the proposed optimization problem, and the complexity of the system can be analyzed based on the received power profile in the presence of human blockages [41]. In the proposed system model, we have first simulated using an infinitely thin obstacle and then using an obstacle having a radius of 0.05m. Linear Regression is applied to the results to develop a predictive algorithm to obtain the location and height of an obstacle from the received power profile. Initially, when no information about the location of the object is available to us, power is allocated equally to all the LED's. Let us then assign the total power to one particular LED at a time while leaving the other 3 LED's with no power and calculate the location error in each of the four scenarios. It makes sense that we should assign more power to the LED, giving the minimum location error. The power allocation algorithm is given by [R30]:

Algorithm 1: Power Allocation Algorithm

Result: Optimum power allocation vector, $\mathbf{\Phi}$
Initial power allocation vector, P
$P_i = \frac{P_t}{4} \ \forall i = \{1, 2, 3, 4\}$
For j = {1,2,3,4}
- Set Power allocation vector, $\mathbf{P^j}$, such that $P_i^j = P_t \ \delta_{ij}$
- Simulate the received power profile of the room and then calculate Location_Error_j

Set,

$$\Phi_i = \frac{\frac{1}{\text{Location\_Error}_i}}{\sum_{j=1}^{4} \frac{1}{\text{Location\_Error}_j}}.$$

where, δ_{ij} is the dirac delta function.

$$\delta_{ij} = \begin{cases} 0 & i \neq j \\ 1 & i = j \end{cases} \tag{34}$$

The performance of this system model can be seen for particular arrangements of objects given in the Fig. 3 From the snapshot, it can be observed that instead of allocating more power to the LED around which some objects are clustered, our allocation scheme allocates more power to the LED from which the average distance of all the objects is lesser. This power allocation algorithm was applied over many iterations, where each iteration has a different number and arrangement of obstacles to improve positioning by optimizing the power allocation to LED's. Over 100 iterations, the power allocation optimization was applied, and the algorithm showed improvements in location accuracy in 20 iterations, with the accuracy remaining unchanged in the rest. We can conclude that there is a saturation point for the accuracy, after which application of the algorithm provides no further improvement. The saturation point varies widely for different arrangements of the objects in the room, and it is difficult to quantify it. The optimization algorithm resulted in an average net improvement of 22.068 % (6- 9 cm) in location accuracy.

B. Optimal LED power allocation

This sub-section shows the results of the proposed optimal LED power allocation scheme to maximize the average data rate with respect to the number of blockages subject to illumination and BER constraints. The realization blockage using MHCP and their respective allotted power to the LEDs has been shown in Fig. 4. Figs. 4(a) and 4(b) show the realization of 3 human blockages and their respective power subject to the total power constraint of 2 W, which is distributed among 4 LEDs using optimal LED power allocation in (11). Similarly, Figs. 4(c) and 4(d) show the realization of 9 human blockages and their respective power allocation.

It can be seen from Fig. 4 that depending on the location of the human blockages, the respective LED power varies in order to fulfill the above constraints. For example, in Figs. 4(c)

This article has been accepted for publication in a future issue of this journal, but has not been fully edited. Content may change prior to final publication. Citation information: DOI 10.1109/JPHOT.2022.3173435, IEEE Photonics Journal

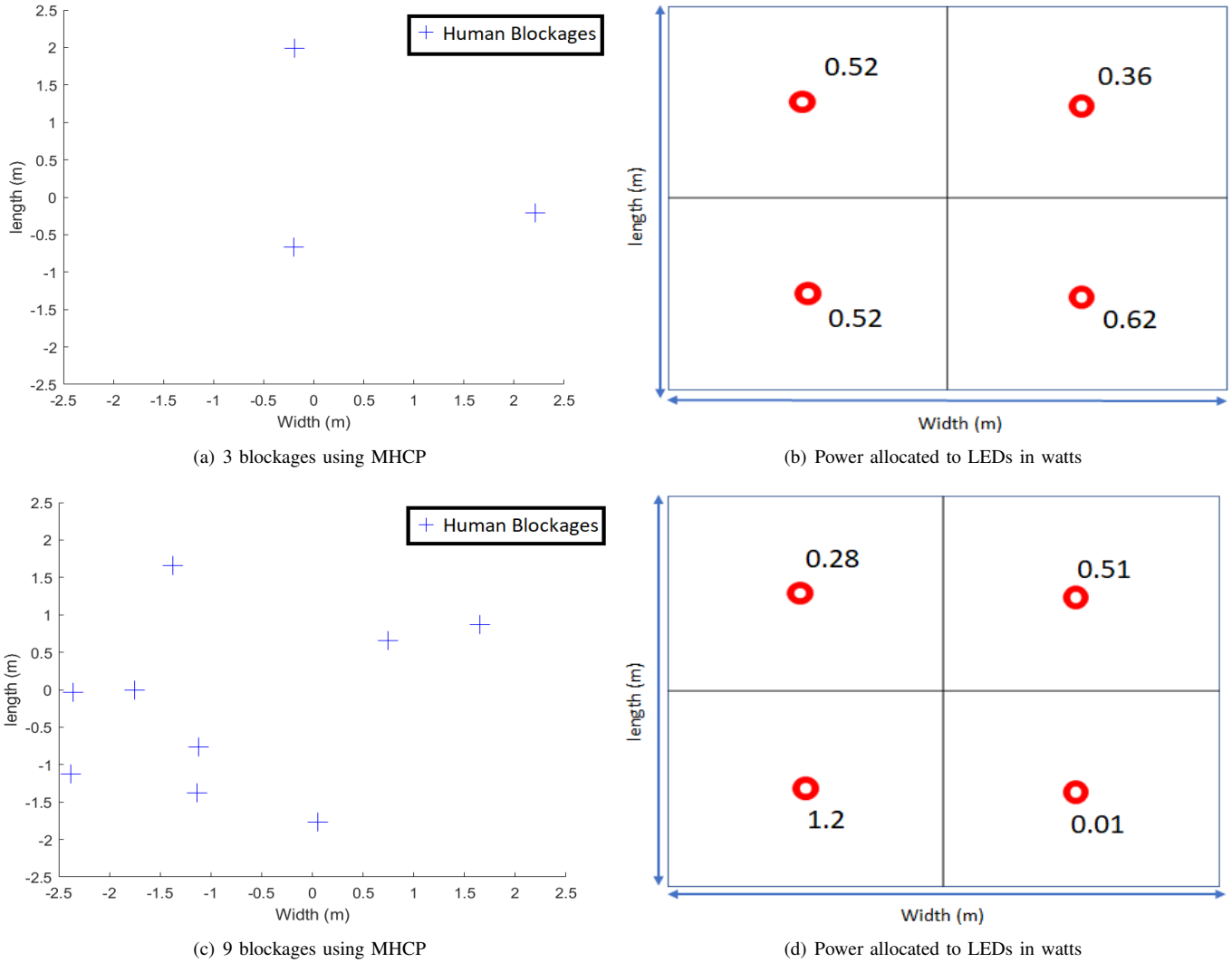

(a) 3 blockages using MHCP

(b) Power allocated to LEDs in watts

(c) 9 blockages using MHCP

(d) Power allocated to LEDs in watts

Fig. 4. Optimal LED power allocation in the presence of blockages with total power of 2 watts

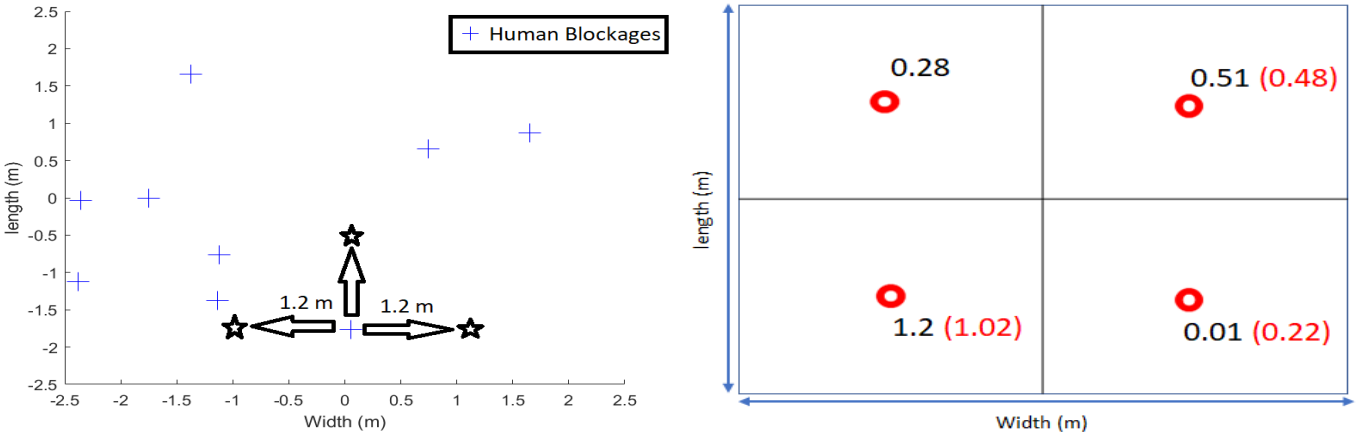

(a) Realization of human blockages

(b) Optimal LED power allocation with respect to shift in blockage location

Fig. 5. Optimal LED power allocation with respect to shift in blockage location (the values in red color shows the updated LED power values due to shift)

and 4(d) with 9 human blockages inside the room, 6 blockages are clustered near the 3rd LED attocell, and the allotted power to the respective LED is 1.2 W. While the 1st and 3rd LEDs have been assigned 0.28 W and 0.51 W of power to serve the

This article has been accepted for publication in a future issue of this journal, but has not been fully edited. Content may change prior to final publication. Citation information: DOI 10.1109/JPHOT.2022.3173435, IEEE Photonics Journal

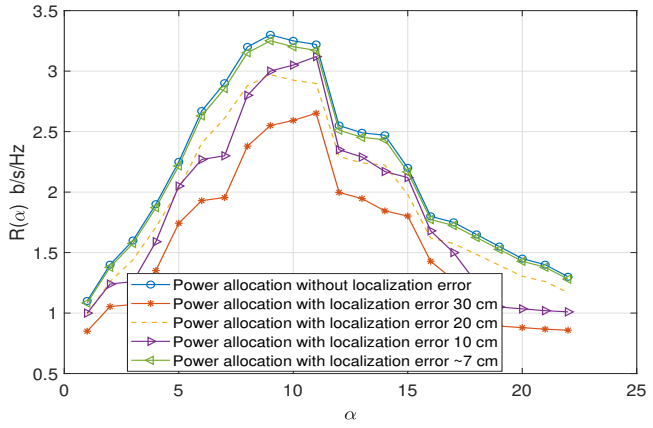

Fig. 6. Convergence of achieved average data rate for different localization error with respect to all possible solution (α)

remaining 3 users. Similarly, the 4th LED has 0 blockages in its attocell, so it has been allotted a minimum required power of 0.1 W to maintain the illumination constraints. Therefore, it can be observed that based on the location information of the users, the respective LED power varies to maximize the data rate subject to the proposed constraints.

Figs. 5(a) and 5(b) show the change in allocated optimal LED power allocation values due to a shift in blockage location. The primary objective is to find the maximum allowed shift in blockage location that will not alter the current LED power allocation which depends on the current location of the blockage as well as the minimum distance required to move out of the coverage area of the respective LED attocell. As shown in Fig. 5(a) that the maximum allowed shift for a given blockage realization is found to be 120 cm.

C. Convergence of the proposed LED power allocation framework

This sub-section shows the convergence of the proposed optimal LED power allocation scheme in the presence of human blockages based on location information. The maximum allowed error in localization with respect to LED and room configuration has also been analyzed. Fig. 6 shows the maximum achievable average data rate for the proposed optimization framework (10) for the given realization of human blockages as shown in Fig. 4(c). The index number of all possible solutions (α) has been chosen such that the maximum average data rate is achieved. It can also be observed from Fig. 6 that as the localization error increases, the maximum achievable data rate decreases as it results in less accurate estimation of the blockage, which will affect the proposed optimization solution. Therefore, we can see that for 4 LEDs configuration with nine blockages in a room size of $5\ \mathrm{m} \times 5\ \mathrm{m} \times 3\ \mathrm{m}$, the maximum allowed localization error is 7 cm with the maximum achieved data rate of 3.28 b/s/Hz. Further, if localization error increases, the achieved data rate decreases. For example, for the localization error of 10 and 20 cm, the maximum achieved data rate reduces to 3.1 and 2.85 b/s/Hz respectively.

D. Optimal LED power allocation framework for 4 and 8 LED configuration with varying room size

Fig. 7 shows the maximum achievable average data rate subject to different localization error for 4 and 8 LED configuration with a room size of $5\ \mathrm{m} \times 5\ \mathrm{m} \times 3\ \mathrm{m}$ and $10\ \mathrm{m} \times 10\ \mathrm{m} \times 3\ \mathrm{m}$.

Fig. 7(a) shows the average achieved data rate for a room size of $5\ \mathrm{m} \times 5\ \mathrm{m} \times 3\ \mathrm{m}$ with 4 and 8 LEDs. As the number of LEDs increases from 4 to 8 LED, the respective maximum allowed localization error decreases from 7 cm to 5 cm. This reduction in localization error is due to the fact that with an increase in the number of LEDs, the separation between the two LEDs decreases the attocell coverage area. Similarly, Fig. 7(a) shows the average achieved data rate for a room size of $10\ \mathrm{m} \times 10\ \mathrm{m} \times 3\ \mathrm{m}$ with 4 and 8 LEDs. It can be observed that the maximum allowed localization error value increases due to increased separation between two LEDs with an increase in room size. The maximum allowed localization error for 4 LED and 8 LED cases are 16 cm and 10 cm respectively. Therefore, it is obvious that increase in the number of LEDs results in a decrease in the maximum allowed localization error with an increase in average data rate. While with the increase in room dimension, the maximum allowed localization error increase for the same number of LEDs with a decrease in the maximum achievable average data rate. Hence, it can be inferred that there exists a trade-off between the maximum achievable average data rate and the maximum allowed localization error and the operator can tune the system as per the requirement.

E. Maximum achieved data rate for different localization error with respect to number of blockages

This sub-section shows the maximum achieved data rate by the proposed scheme in the presence of human blockages for varying localization error subject to fulfilling both illumination and BER constraints for a room size of $5\ \mathrm{m} \times 5\ \mathrm{m} \times 3\ \mathrm{m}$. Fig. 8 shows the maximum achievable data rate as a function of localization error for increasing number of blockages for 4 and 8 LED configurations. It can be seen that as the number of human blockages increases, the maximum achievable data rate decreases along with maximum localization error for 4 LED configuration as shown in Fig. 8(a). For example, with 2 blockages and an allowed localization error of 5 cm, the maximum achieved data rate is 3.25 b/s/Hz. For the same number of blockages with an increase in localization error to 20 cm, the maximum achieved data rate is reduced to 2.75 b/s/Hz. Similarly, in Fig. 8(b) with 8 LED configurations, the effect is nearly the same. It can be observed that with 2 blockages and with allowed localization error of 5 cm, the maximum achievable data rate is 3.65 b/s/Hz, while for the same number of blockages and increase in localization error to 20 cm, the maximum achievable data rate reduces to 3.05 b/s/Hz. It is due to the fact that for 8 LED configuration, there is less separation between the LEDs, the transmit power is more uniformly distributed but at the same time, the localization error also increases due to more overlapping regions in their respective attocell.

This article has been accepted for publication in a future issue of this journal, but has not been fully edited. Content may change prior to final publication. Citation information: DOI 10.1109/JPHOT.2022.3173435, IEEE Photonics Journal

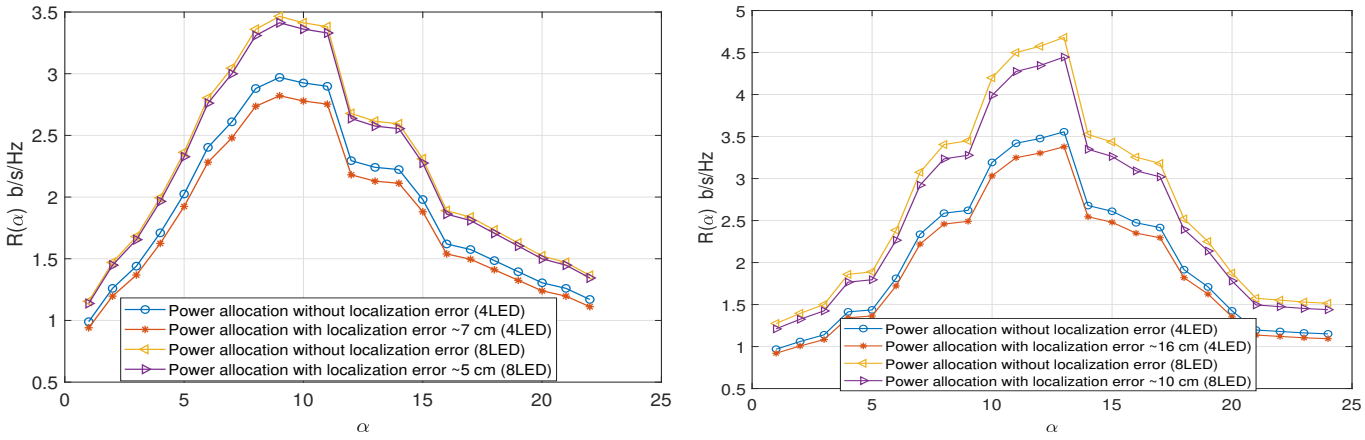

(a) Achieved average data rate with 4 and 8 LEDs for room $5\ \mathrm{m} \times 5\ \mathrm{m} \times 3\ \mathrm{m}$ (b) Achieved average data rate with 4 and 8 LEDs for room $10\ \mathrm{m} \times 10\ \mathrm{m} \times 3\ \mathrm{m}$

Fig. 7. Achieved average data rate with localization error for 4 and 8 LEDs and two room dimensions

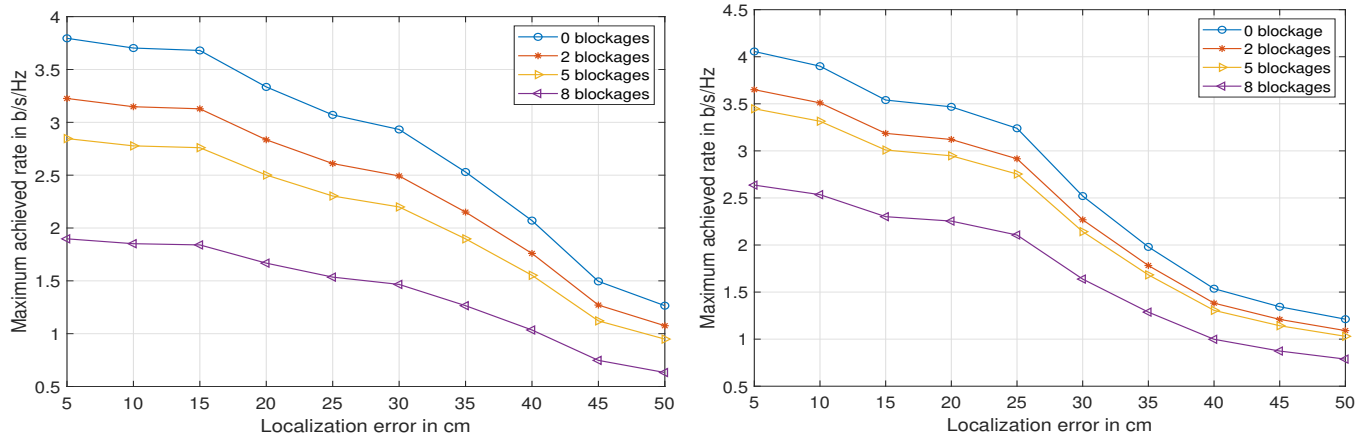

(a) Maximum achieved data rate with 4 LEDs

(b) Maximum achieved data rate with 8 LEDs

Fig. 8. Maximum achieved data rate for different localization error with 4 and 8 LEDs

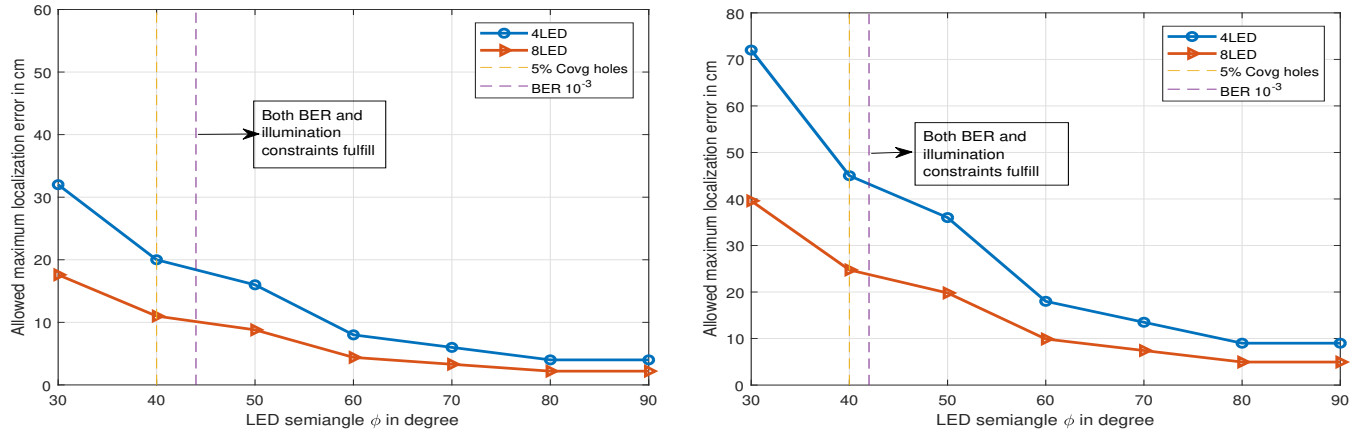

(a) $5\ \mathrm{m} \times 5\ \mathrm{m} \times 3\ \mathrm{m}$

(b) $10\ \mathrm{m} \times 10\ \mathrm{m} \times 3\ \mathrm{m}$

Fig. 9. Maximum allowed Localization error versus the LED semiangle with 4 and 8 LED configuration

From the above results, it can be inferred that the maximum achieved data rate decreases with the increase in localization error and the number of blockages. Hence, depending on the requirement of the system with a given number of blockages

This article has been accepted for publication in a future issue of this journal, but has not been fully edited. Content may change prior to final publication. Citation information: DOI 10.1109/JPHOT.2022.3173435, IEEE Photonics Journal

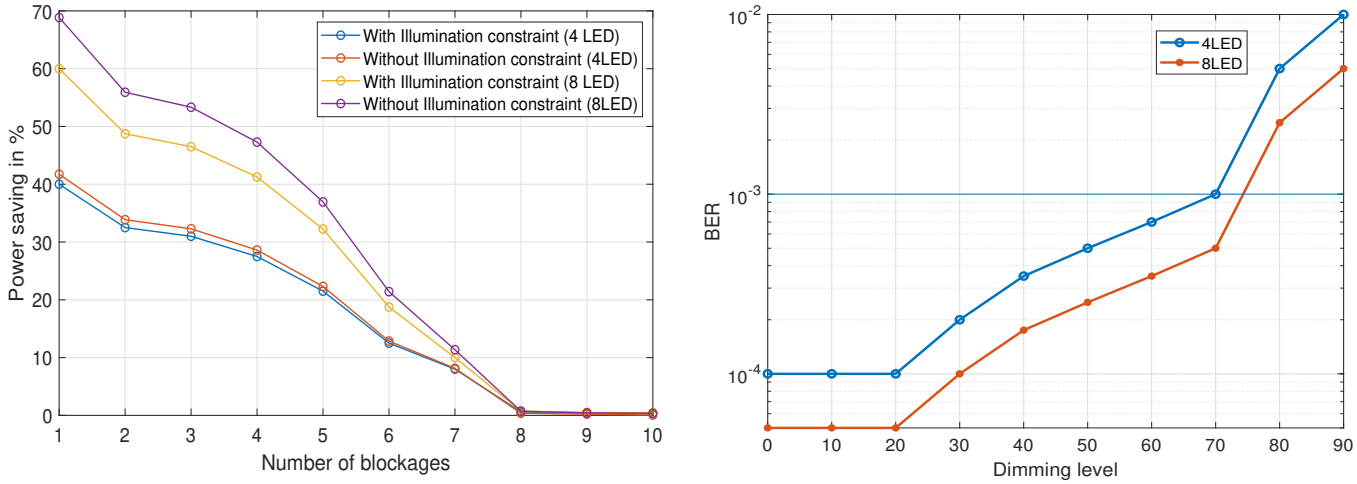

(a) Power saving with respect to number of blockages

(b) Achieved BER with respect to dimming

Fig. 10. Power saving and dimming performance with and without illumination constraints

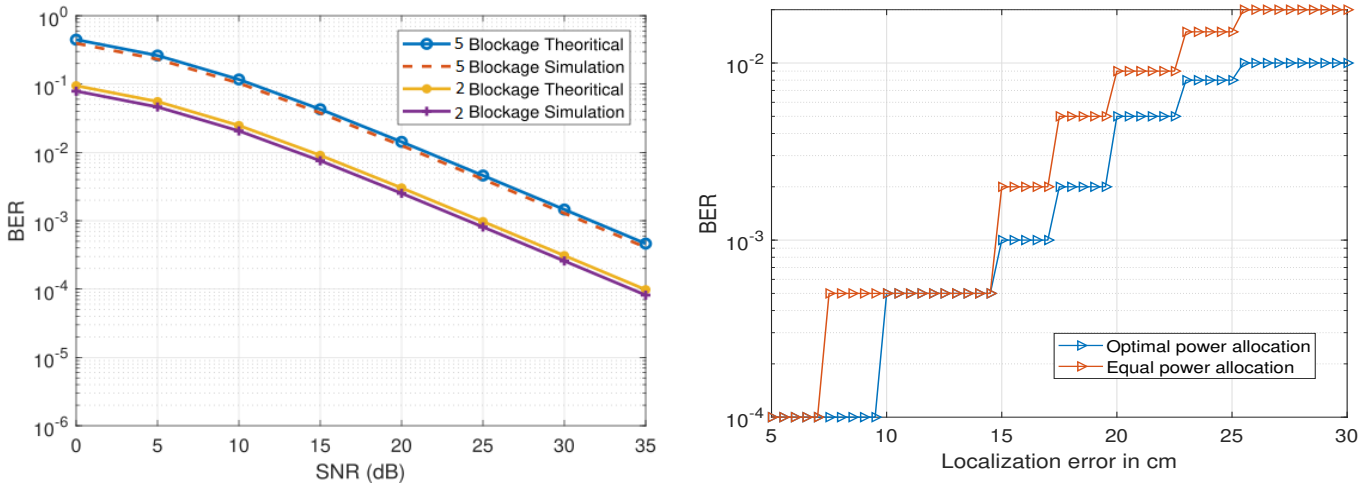

(a) BER performance with blockages

(b) BER versus localization error with 5 human blockages

Fig. 11. BER Performance

and errors in the localization, one can deploy either the 4 or 8 LED configuration.

F. Effect of LED semiangle in the maximum allowed localization error

In this sub-section, The effect of LED semiangle on the maximum allowed error in localization has been shown in Fig. 9. The increased LED semiangle results in an increase in attocell size. The increase in attocell size leads to more overlapping regions among LEDs and, affects the maximum allowed localization error. Figs. 9(a) and 9(b) show the maximum allowed localization error with 4 and 8 LEDs for a room size of $5\ \mathrm{m} \times 5\ \mathrm{m} \times 3\ \mathrm{m}$ and $10\ \mathrm{m} \times 10\ \mathrm{m} \times 3\ \mathrm{m}$ respectively. In both cases, the maximum allowed localization error decreases with an increase in LED semiangle. For the case of $5\ \mathrm{m} \times 5\ \mathrm{m} \times 3\ \mathrm{m}$ room size, the minimum required LED semiangle is 44° with maximum allowed localization error of 10 cm and 18 cm while maintaining the illumination and BER constraints for 4 and 8 LEDs respectively. Similarly, for the case of room size of $10\ \mathrm{m} \times 10\ \mathrm{m} \times 3\ \mathrm{m}$ minimum required LED semiangle is 42.8° with maximum allowed localization error of 22 cm and 43 cm for 4 LED and 8 LED respectively. It is worth mentioning that wider LED semiangle results in more uniform received power and better BER across the room while decreasing the maximum allowed localization error and vice versa. Therefore, it can be inferred that there is a trade-off between the allowed maximum localization error versus the illumination and BER constraints. Wider LED semiangle satisfies the illumination and BER constraints with good margin but suffers in maximum allowed localization error and vice versa.

This article has been accepted for publication in a future issue of this journal, but has not been fully edited. Content may change prior to final publication. Citation information: DOI 10.1109/JPHOT.2022.3173435, IEEE Photonics Journal

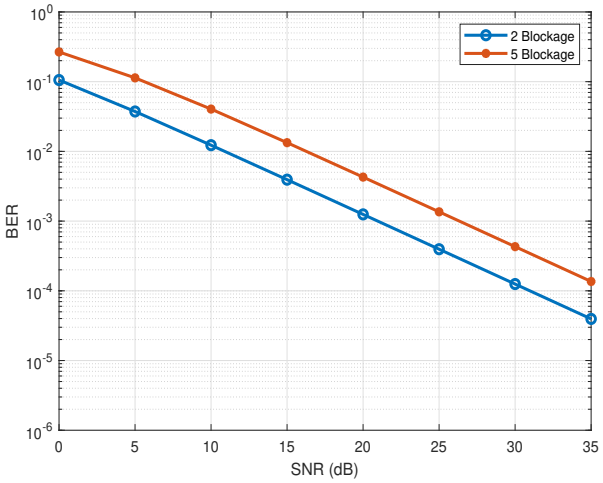

(a) BER performance with blockages using DCO-OFDM

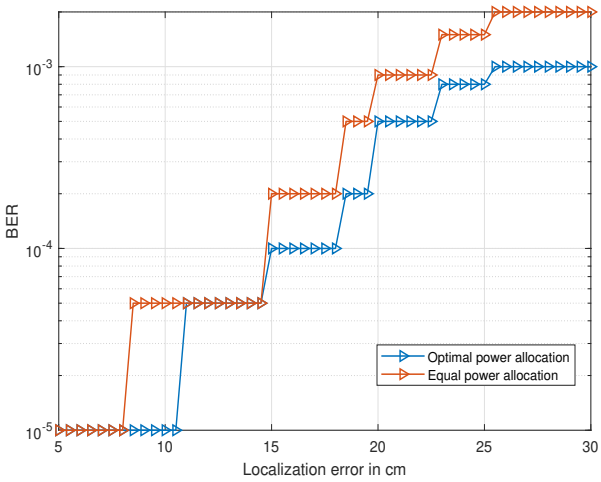

(b) BER versus localization error with 5 human blockages using DCO-OFDM

Fig. 12. BER Performance with DCO-OFDM

G. Power saving with and without illumination constraint under the effect of dimming

In this sub-section, we have shown the maximum possible power saving for the proposed optimal LED power allocation scheme with and without illumination constraints for 4 and 8 LEDs configuration for a room size of $5\ \mathrm{m} \times 5\ \mathrm{m} \times 3\ \mathrm{m}$. The power-saving is calculated using the (22) subject to the number of blockages. In order to calculate the power saving in percentage in the denominator, we have taken the constant power P_T. The formula for the percentage of power-saving P_S is written as:

$$P_S = \frac{\max\limits_{N_B} \ [P_T - P_A]}{P_T} \times 100, \tag{35}$$

Denominator P_T is fixed for all lighting scenarios to maintain the fair comparison with constant power. We have taken 2 Watt constant power for 4 and 8 LEDs arranged in rectangular configurations. Fig. 10(a) shows the power saving with varying number of human blockages for with and without illumination constraints for the optimization problem formulated in (24). It can be seen that for 4 LED case with one blockage, the maximum power saving achieved with and without illumination constraint is nearly the same which is approximately 40 %. Further, it is observed that the power saving decreases with an increase in the number of blockages. While for the case of 8 LED, the maximum power saving without any blockages and illumination constraint is 70 %, and with illumination constraint, it is reduced to 60 %. It is observed that the power saving decreases with an increase in the number of blockages for both cases. It goes to zero with blockages more than 7. For the given room size, this is the maximum number of blockages that can be served. Therefore, it can be inferred that for a given room size of $5\ \mathrm{m} \times 5\ \mathrm{m} \times 3\ \mathrm{m}$, the maximum allowed human blockages are ≤ 7 to save the power.

In the VLC system, the illumination due to LED should be adjusted based on the user's need as well as for saving energy [42], [43]. Fig. 10(b) shows the achieved BER with respect to the dimming percentage for 4 and 8 LEDs with 5 blockages. As the dimming percentage increases, the respective BER starts increasing for both cases. As the dimming percentage increases, the received power decreases, which results in an error in localization, and the effective SNR decreases. It can be seen that for 4 LED case, the maximum allowed dimming is 70 %, while for 8 LED case, it is approximately 75 %.

H. BER performance with optimal LED power allocation

This sub-section shows the BER performance of the proposed system with equal and optimal power allocation schemes. Fig. 11(a) shows the BER performance in the presence of human blockages. The derived BER expressions and the simulation results are in close agreement, which validates the mathematical derivations and justifies the approximations in (33). Fig. 11(b) shows the BER with respect to localization error in estimation with equal power allocation and proposed optimal LED power allocation schemes. It can be seen that as the localization error increases, the BER decreases in both cases. However, it is interesting to observe that the system with optimal LED power allocation can tolerate more error in localization as compared to equal power allocation scheme for the same BER values. We have also plotted the BER performance results with blockages using DCO-OFDM as shown in Fig. 12 and compared it with standard OOK modulation as shown in Fig. 11.

TABLE II
PERFORMANCE COMPARISON

Modulation Scheme	**SNR for BER of** $10^{-}3$)	**Localization Error**
OOK with 2B	23 dB	9 cm
DCO-OFDM with 2B	20 dB	11 cm
OOK with 5B	30 dB	7 cm
DCO-OFDM with 5B	27 dB	9 cm

This article has been accepted for publication in a future issue of this journal, but has not been fully edited. Content may change prior to final publication. Citation information: DOI 10.1109/JPHOT.2022.3173435, IEEE Photonics Journal

It can be seen from Fig. 11(a) and Fig. 12(a) the BER performance with blockages using OOK and DCO-OFDM, respectively using location information. To achieve the BER of 10^{-3} with 2 blockages, the SNR required using OOK is approximately 23 dB, whereas, in the case of DCO-OFDM, it is around 20 dB. Similarly, for 5 blockages, the required SNR is 30 dB, whereas, in the case of DCO-OFDM, it is approximately 27 dB. DCO-OFDM provides the gain of 3 dB with respect to OOK. It is because, with DCO OFDM, the data stream is parallelized and sent through orthogonal sub-carriers. Each sub-stream can be modulated using a high-order modulation such as phase-shift keying (PSK) or quadrature amplitude modulation (QAM). Furthermore, external narrow-band interference will most probably impact only a limited number of subcarriers while the other subcarriers will remain unaltered, which in turn leads to better-received power and better error rate performances [44].

Similarly, Fig. 11(b) and Fig. 12(b) show the BER versus the localization error with equal and optimal power allocation scheme using OOK and DCO-OFDM, respectively. As the optimum power allocation vector is calculated using received power as a reference, the LED optimal power allocation vector in a change in modulation scheme remains the same. Only the BER ranges widen for DCO-OFDM in respect of the standard OOK scheme. For example, with DCO-OFDM, we can maintain BER of 10^{-5} up to the localization error of 11 cm, while in the case of OOK, it is around 9 cm. We can say that with higher-order modulation schemes such as DCO-OFDM, we can reduce the range of SNR with respect to the required BER performance as shown in Table II.

I. BER performance with random device orientation

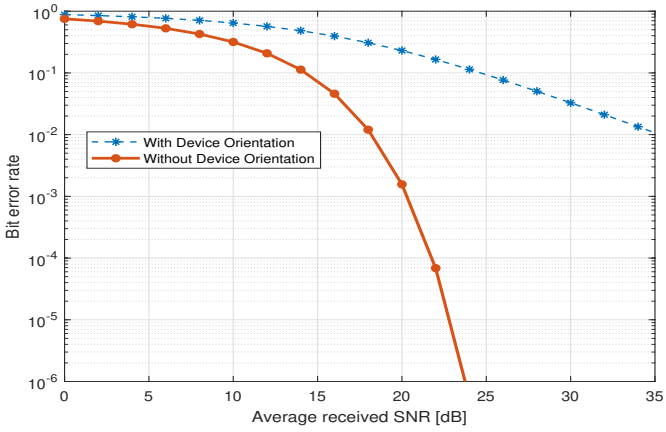

Fig. 13. BER performance with and without device orientation

In this subsection, we have considered the impact of random orientation in their analysis, for instance, and references therein [8], [45]. All these works signify the importance of incorporating user equipment (UE) orientation. In the previous BER performance, we are considering that the PD is facing directly upward for ease of analysis. The above assumption has been made to simplify the proper orientation model and make the analysis tractable. To address the effect of random device orientation on the proposed system, we have plotted the BER performance considering the random device orientation of the receiver and compared it without device orientation, as shown in Fig. 13. It can be seen that by considering random device orientation, the BER performance degraded even with the location information. It is due to the fact that the acquiring location information does not confirm the direction of the receiver, and the random device orientation results in self blockage, sometimes affecting the received power.

VI. CONCLUSION

In this paper, a location-assisted VLC system with human blockages has been analyzed. We have proposed the optimal LED power allocation scheme based on location information, resulting in a better indoor communication system in terms of BER, achieved data rate, and illumination across the room. The closed-form expression for BER with MHCP is derived for the optimal LED power allocation schemes with human blockages. The analytical results are in close agreement with the simulation results, which validates the analytical framework proposed in the article. The proposed work also established that with the proposed optimal LED power allocation scheme can support up to 70 % and 75 % dimming range of visible light with 4 and 8 LED respectively. Further, we have also proposed an optimization framework to maximize power saving with and without dimming among the LEDs while satisfying the communication constraints. Further, to see the effect of a high rate modulation scheme in the proposed system model, we have analyzed the BER performance and the localization error with DCO-OFDM and human blockage.

This work also analyzed the maximum allowed localization error for varying room sizes and the number of LEDs with respect to blockages. In addition, the proposed work also studied the trade-off between the achieved data rate with respect to allowed localization error as a function of LED semiangle. It is shown that for a room size of $5\ \mathrm{m}\times5\ \mathrm{m}\times3\ \mathrm{m}$, the minimum required LED semiangle is 44° for 4 and 8 LED configuration and for room size of $10\ \mathrm{m}\times10\ \mathrm{m}\times3\ \mathrm{m}$, it is 42.8° to maintain both illumination and BER constraints. Furthermore, through the obtained results it is observed that maximum achieved data rate is subject to varying localization error and is a function of number of human blockages inside the room. Further, the proposed framework can be easily extended for other used cases such as factories and shopping malls with different lighting requirements. The proposed optimization problem can be modified with the required constraints to provide both illumination and communication.

REFERENCES

[1] E. A. Jarchlo, E. Eso, H. Doroud, A. Zubow, F. Dressler, Z. Ghassemlooy, B. Siessegger, and G. Caire, "Fdla: A novel frequency diversity and link aggregation solution for handover in an indoor vehicular VLC network," *IEEE Transactions on Network and Service Management*, vol. 18, no. 3, pp. 3556–3566, 2021.

[2] L. Shi, D. Shi, X. Zhang, B. Meunier, H. Zhang, Z. Wang, A. Vladimirescu, W. Li, Y. Zhang, J. Cosmas, K. Ali, N. Jawad, R. Zetik, E. Legale, M. Satta, J. Wang, and J. Song, "5G internet of radio light positioning system for indoor broadcasting service," *IEEE Transactions on Broadcasting*, vol. 66, no. 2, pp. 534–544, 2020.

[3] J. J. Gimenez, J. L. Carcel, M. Fuentes, E. Garro, S. Elliott, D. Vargas, C. Menzel, and D. Gomez-Barquero, "5G new radio for terrestrial broadcast: A forward-looking approach for nr-mbms," *IEEE Transactions on Broadcasting*, vol. 65, no. 2, pp. 356–368, 2019.

[4] R. Raj and A. Dixit, "Outage analysis and reliability enhancement of hybrid VLC-RF networks using cooperative Non-orthogonal multiple access," *IEEE Transactions on Network and Service Management*, vol. 18, no. 4, pp. 4685–4696, 2021.

[5] J. Armstrong, Y. A. Sekercioglu, and A. Neild, "Visible light positioning: a roadmap for international standardization," *IEEE Communications Magazine*, vol. 51, no. 12, pp. 68–73, 2013.

[6] S. Bastiaens, S. K. Goudos, W. Joseph, and D. Plets, "Metaheuristic optimization of LED locations for visible light positioning network planning," *IEEE Transactions on Broadcasting*, pp. 1–15, 2021.

[7] Z. Ghassemlooy, S. Arnon, M. Uysal, Z. Xu, and J. Cheng, "Emerging optical wireless communications-advances and challenges," *IEEE journal on selected areas in communications*, vol. 33, no. 9, pp. 1738–1749, 2015.

[8] M. D. Soltani, X. Wu, M. Safari, and H. Haas, "Bidirectional user throughput maximization based on feedback reduction in LiFi networks," *IEEE Transactions on Communications*, vol. 66, no. 7, pp. 3172–3186, 2018.

[9] H. Haas, L. Yin, Y. Wang, and C. Chen, "What is lifi?" *Journal of lightwave technology*, vol. 34, no. 6, pp. 1533–1544, 2015.

[10] M. Obeed, A. M. Salhab, M.-S. Alouini, and S. A. Zummo, "On optimizing VLC networks for downlink multi-user transmission: A survey," *IEEE Communications Surveys & Tutorials*, vol. 21, no. 3, pp. 2947–2976, 2019.

[11] L. E. M. Matheus, A. B. Vieira, L. F. Vieira, M. A. Vieira, and O. Gnawali, "Visible light communication: concepts, applications and challenges," *IEEE Communications Surveys & Tutorials*, vol. 21, no. 4, pp. 3204–3237, 2019.

[12] M. Biagi, N. B. Hassan, K. Werfli, T.-C. Bui, and Z. Ghassemlooy, "Analysis and demonstration of quasi trace orthogonal space time block coding for visible light communications," *IEEE Access*, vol. 8, pp. 77 164–77 170, 2020.

[13] H. Elgala, R. Mesleh, and H. Haas, "Indoor optical wireless communication: potential and state-of-the-art," *IEEE Communications Magazine*, vol. 49, no. 9, pp. 56–62, 2011.

[14] F. Miramirkhani and M. Uysal, "Channel modeling and characterization for visible light communications," *IEEE Photonics Journal*, vol. 7, no. 6, pp. 1–16, 2015.

[15] J. Grubor, S. Randel, K.-D. Langer, and J. W. Walewski, "Broadband information broadcasting using LED-based interior lighting," *Journal of Lightwave technology*, vol. 26, no. 24, pp. 3883–3892, 2008.

[16] A. Singh, G. Ghatak, A. Srivastava, V. A. Bohara, and A. K. Jagadeesan, "Performance analysis of indoor communication system using off-the-shelf LEDs with human blockages," *IEEE Open Journal of the Communications Society*, vol. 2, pp. 187–198, 2021.

[17] I. Din and H. Kim, "Energy-efficient brightness control and data transmission for visible light communication," *IEEE photonics technology letters*, vol. 26, no. 8, pp. 781–784, 2014.

[18] P. M. Butala, H. Elgala, and T. D. C. Little, "Svd-vlc: A novel capacity maximizing vlc mimo system architecture under illumination constraints," in *2013 IEEE Globecom Workshops (GC Wkshps)*, 2013, pp. 1087–1092.

[19] G. Simon, G. Zachár, and G. Vakulya, "Lookup: Robust and accurate indoor localization using visible light communication," *IEEE Transactions on Instrumentation and Measurement*, vol. 66, no. 9, pp. 2337–2348, 2017.

[20] A.-C. Anastou, K. K. Delibasis, A.-A. A. Boulogeorgos, H. G. Sandalidis, A. Vavoulas, and S. K. Tasoulis, "A low complexity indoor visible light positioning method," *IEEE Access*, vol. 9, pp. 57 658–57 673, 2021.

[21] A. Adnan-Qidan, M. Morales-Céspedes, and A. G. Armada, "Load balancing in hybrid vlc and rf networks based on blind interference alignment," *IEEE Access*, vol. 8, pp. 72 512–72 527, 2020.

[22] M. Obeed, A. M. Salhab, M.-S. Alouini, and S. A. Zummo, "On optimizing vlc networks for downlink multi-user transmission: A survey," *IEEE Communications Surveys Tutorials*, vol. 21, no. 3, pp. 2947–2976, 2019.

[23] J. Xu, H. Shen, W. Xu, H. Zhang, and X. You, "LED-assisted three-dimensional indoor positioning for multiphotodiode device interfered by multipath reflections," in *2017 IEEE 85th Vehicular Technology Conference (VTC Spring)*, 2017, pp. 1–6.

[24] F. Alam, N. Faulkner, and B. Parr, "Device-free localization: A review of non-rf techniques for unobtrusive indoor positioning," *IEEE Internet of Things Journal*, vol. 8, no. 6, pp. 4228–4249, 2021.

[25] L. Bai, Y. Yang, C. Feng, C. Guo, and B. Jia, "Novel visible light communication assisted perspective-four-line algorithm for indoor localization," in *GLOBECOM 2020 - 2020 IEEE Global Communications Conference*, 2020, pp. 1–6.

[26] E. W. Lam and T. D. C. Little, "Zone-based positioning using trust beacons, angle diversity, and optical wireless communications," in *2020 IEEE International Conference on Communications Workshops (ICC Workshops)*, 2020, pp. 1–6.

[27] S. Cincotta, A. Neild, and J. Armstrong, "Luminaire reference points (lrp) in visible light positioning using hybrid imaging-photodiode (hip) receivers," in *2019 International Conference on Indoor Positioning and Indoor Navigation (IPIN)*, 2019, pp. 1–8.

[28] M. Dehghani Soltani, X. Wu, M. Safari, and H. Haas, "Access point selection in li-fi cellular networks with arbitrary receiver orientation," in *2016 IEEE 27th Annual International Symposium on Personal, Indoor, and Mobile Radio Communications (PIMRC)*, 2016, pp. 1–6.

[29] X. Wu, M. Safari, and H. Haas, "Bidirectional allocation game in visible light communications," in *2016 IEEE 83rd Vehicular Technology Conference (VTC Spring)*, 2016, pp. 1–5.

[30] R. Zhang, Y. Cui, H. Claussen, H. Haas, and L. Hanzo, "Anticipatory association for indoor visible light communications: Light, follow me!" *IEEE Transactions on Wireless Communications*, vol. 17, no. 4, pp. 2499–2510, 2018.

[31] R. Jiang, Q. Wang, H. Haas, and Z. Wang, "Joint user association and power allocation for cell-free visible light communication networks," *IEEE Journal on Selected Areas in Communications*, vol. 36, no. 1, pp. 136–148, 2018.

[32] C. Chen, D. A. Basnayaka, and H. Haas, "Downlink performance of optical attocell networks," *Journal of Lightwave Technology*, vol. 34, no. 1, pp. 137–156, 2016.

[33] S. A. Zakerian, S. Yazdanirad, S. Gharib, K. Azam, and A. Zare, "The effect of increasing the illumination on operators' visual performance in the control-room of a combined cycle power plant," *Annals of occupational and environmental medicine*, vol. 30, no. 1, pp. 1–7, 2018.

[34] E. M. De Korte, M. Spiekman, L. Hoes-van Oeffelen, B. van der Zande, G. Vissenberg, G. Huiskes, and L. F. Kuijt-Evers, "Personal environmental control: effects of pre-set conditions for heating and lighting on personal settings, task performance and comfort experience," *Building and Environment*, vol. 86, pp. 166–176, 2015.

[35] Z. Feng, C. Guo, Z. Ghassemlooy, and Y. Yang, "The spatial dimming scheme for the mu-mimo-ofdm vlc system," *IEEE Photonics Journal*, vol. 10, no. 5, pp. 1–13, 2018.

[36] B. Matérn, *Spatial variation*. Springer Science & Business Media, 2013, vol. 36.

[37] S. N. Chiu, D. Stoyan, W. S. Kendall, and J. Mecke, *Stochastic geometry and its applications*. John Wiley & Sons, 2013.

[38] L. Wu, Y. Shen, Z. Zhang, J. Dang, H. Liu, and J. Wang, "Receiver algorithms for single-carrier osm based high-rate indoor visible light communications," *IEEE Transactions on Wireless Communications*, vol. 19, no. 2, pp. 1113–1126, 2020.

[39] S. Boyd, S. P. Boyd, and L. Vandenberghe, *Convex optimization*. Cambridge university press, 2004.

[40] I. Neokosmidis, T. Kamalakis, J. W. Walewski, B. Inan, and T. Sphicopoulos, "Impact of nonlinear LED transfer function on discrete multitone modulation: Analytical approach," *Journal of Lightwave Technology*, vol. 27, no. 22, pp. 4970–4978, 2009.

[41] A. Chakraborty, A. Singh, V. A. Bohara, and A. Srivastava, "A visible light communication based predictive system for the height and location estimation of an obstacle," in *2020 IEEE International Conference on Advanced Networks and Telecommunications Systems (ANTS)*. IEEE, 2020, pp. 1–6.

[42] Z. Feng, G. Papageorgiou, Q. Gao, A. F. Atya, S. V. Krishnamurthy, and G. Chen, "Performance of visible light communications with dimming controls," in *Wireless Communications and Networking Conference (WCNC), 2014 IEEE*. IEEE, 2014, pp. 1756–1761.

[43] Y. Yang, Z. Zeng, J. Cheng, and C. Guo, "An enhanced DCO-OFDM scheme for dimming control in visible light communication systems," *IEEE Photonics Journal*, vol. 8, no. 3, pp. 1–13, 2016.

[44] B. Béchadergue, W.-H. Shen, and H.-M. Tsai, "Comparison of OFDM and OOK modulations for vehicle-to-vehicle visible light communication in real-world driving scenarios," *Ad Hoc Networks*, vol. 94, p. 101944, 2019.

[45] M. D. Soltani, Z. Zeng, I. Tavakkolnia, H. Haas, and M. Safari, "Random receiver orientation effect on channel gain in lifi systems," in *2019 IEEE Wireless Communications and Networking Conference (WCNC)*. IEEE, 2019, pp. 1–6.